Available online at www.sciencedirect.com
ScienceDirect
Remote Sensing of Environment 107 (2007) 2 – 11
Remote Sensing of Environment
www.elsevier.com/locate/rse

The MISR radiometric calibration process

Carol J. Bruegge [a,*], David J. Diner [a], Ralph A. Kahn [a], Nadine Chrien [b], Mark C. Helmlinger [c], Barbara J. Gaitley [a], Wedad A. Abdou [a]

[a] Jet Propulsion Laboratory, California Institute of Technology, Pasadena, California, United States
[b] Instrument Design Engineering Associates, Brea, California, United States
[c] Northrop Grumman Space Technologies, El Segundo, California, United States

Received 8 March 2006; received in revised form 14 July 2006; accepted 17 July 2006

Abstract

One important objective of the Multi-angle Imaging SpectroRadiometer (MISR) is retrieving global aerosol loading and microphysical properties. Accuracy depends on many factors, including the availability of a complete catalog of particle types with their associated size distributions, shapes, single-scattering albedos, vertical profiles, and spectral radiative characteristics. Co-equal to this need is the availability of a well-designed, well-characterized instrument, with a calibration that is maintained post-launch. This allows accurate radiance and retrieval products to be made, adjusting for instrument changes. MISR performance has been intensively studied throughout the design, pre-flight, and post-launch mission phases. To establish the absolute radiometric scale, annual vicarious calibration (VC) exercises have been conducted. In addition, an on-board-calibrator (OBC) allows more frequent testing of camera degradations. Together, the VC and OBC processes have allowed MISR to achieve an absolute calibration uncertainty of 4% or better (1σ confidence level) for bright land targets. Additional fine-tunings have been made following analysis of lunar-view campaign data, and from a statistical analysis of Earth observations. These studies led to slight camera-to-camera adjustments, which are important in improving the aerosol retrieval process. Validation of the response at the lower end of the dynamic range has also been accomplished using a dark-water study. With these studies complete, MISR calibration is now in an operational mode, and data users can be assured the resulting data products are stable with time. Such records meet the needs of a program designed to support climate change and provide long-term monitoring of the Earth's atmosphere and radiative fluxes.

Keywords: Radiometric calibration; MISR

1. Introduction

1.1. Science drivers to accurate radiometry

MISR aerosol optical depth uncertainty requirements have been specified as 0.05 or 20%, which ever is larger, under average, cloud-free viewing conditions. Further, there exists a goal to achieve 0.01 to 0.02 uncertainty in the future. The latter is comparable to the best surface-based instrument uncertainties, but can be reached in some cases by creating monthly averages that reduce instantaneous retrieval noise. MISR measurements distinguish spherical from non-spherical particles, separate two to four compositional groups based on indices of refraction, and identify three to four distinct size groups between 0.1 and 2.0 μm characteristic radius at most latitudes (Kahn et al., 1998, 2001; Kalashnikova & Kahn, in press). Over deep water, the MISR aerosol retrieval algorithm uses the 672 and 866 nm bands, similar to other sensors that take advantage of the very low surface reflectance at these wavelengths. At high optical depths, data from the 446 and 558 nm bands are also incorporated. An advantage of multi-angle observations is that aerosol retrievals over water are possible even when some cameras are affected by sun glint. Over land, aerosol retrievals are complicated by the large variability in surface bidirectional reflectance factor (BRF), and that ground-reflectance is high for much of the Earth, including desert and urban areas that are major aerosol source regions. The MISR land aerosol algorithm models the shape of the surface BRF as a linear sum of angular empirical orthogonal functions derived directly from the image data, making use of spatial contrasts to separate the surface and atmospheric signals (Diner et al., 2001, 2005; Martonchik et al., 2002). Aerosols are

* Corresponding author.
E-mail address: Carol.J.Bruegge@jpl.nasa.gov (C.J. Bruegge).

0034-4257/$ - see front matter © 2007 Elsevier Inc. All rights reserved.
doi:10.1016/j.rse.2006.07.024

detected by virtue of their effect on the angular variation in the observed spectral radiance, rather than by their effect on absolute brightness (which does play a role in the dark-water algorithm).

To achieve the scientific objectives, MISR calibration requirements specify 3% absolute and 1% band and camera-relative calibrations, for bright targets (at equivalent reflectances of one). Here we define top-of-atmosphere equivalent reflectance as $\rho = \pi L / E_0$, where L is the top-of-atmosphere radiance within a given MISR band, and E_0 is the MISR total-band-weighted exo-atmosphere solar irradiance. Requirements at the low end of the dynamic range specify a 10% absolute uncertainty at a scene equivalent reflectance of 0.02. For dark-water scenes having aerosol optical depths on the order 0.2 or less at mid-visible wavelengths, the equivalent reflectance typically falls below 7%. The aerosol optical depth calibration uncertainty requirement is 0.02 or better, in all channels. This is the more demanding of the two requirements, and is at the cutting edge of current capabilities.

2. MISR instrument

MISR was launched into polar orbit on December 18, 1999 aboard the NASA Earth Observing System (EOS) Terra spacecraft. MISR makes near-simultaneous measurements at nine view angles spread out in the forward (f) and aft (a) directions along the flight path, using nine separate push-broom cameras observing Earth at 70° (cameras Df and Da), 60° (Cf and Ca), 46° (Bf and Ba), 26° (Af and Aa), and nadir (An). Each camera contains four spectral bands centered at 447, 558, 672, and 867 nm. For each of these the spectral band is Gaussian in shape. This profile, used in conjunction with a Lyot depolarizer, provides depolarization of the incoming light to within an uncertainty of ±1%. MISR obtains global coverage between ±82° latitude in 9 days, with spatial sampling per pixel between 275 m and 1.1 km, depending on channel and data acquisition mode. The instrument systematically covers a range of airmass factors from 1–3, and in mid-latitudes, samples scattering angles extending from about 60–160°. The analog readouts from the charge-coupled device (CCD) detectors in the camera focal planes are digitized to 14 bits. Thermoelectric coolers and focal plane heaters are used to maintain stable detector temperatures of −5.0±0.1 °C.

2.1. On-board calibrator

The MISR radiometric response scale is established using an on-board calibrator (OBC), as well as by vicarious calibration experiments (Abdou et al., 2002; Bruegge et al., 2002). The strength of the OBC is its ability to conveniently and frequently test the camera response. Calibrations using the OBC are conducted once every 2 months. The OBC, depicted in Fig. 1, consists of two Spectralon diffuser panels, and six sets of photodiode detectors. The latter measure solar-reflected light from the panels, and provide the camera-incident radiance. These are regressed against the camera digital number (DN) output, in order to provide the radiometric response for each of the 1504 CCD detector elements per line array, nine cameras, and four spectral bands per camera. One such photodiode is set on a goniometric arm to monitor changes in panel bidirectional reflectance factor (BRF).

Although OBC system degradation can occur, MISR experiment accuracy has benefited from the stability of the calibrator with time. Pre-launch testing (Bruegge et al., 1993, 2001; Stiegman et al., 1993) established Spectralon preparation and handling procedures that would reduce the risk of on-orbit degradation. Hydrocarbon contaminants, such as machining oils introduced during manufacture or testing, were shown to cause degradation when exposed to on-orbit vacuum ultraviolet light. With this information at hand, the MISR Spectralon panels were vacuum-baked, following laboratory reflectance testing, to remove any such contaminants. In addition, the original panels, in place during instrument integration and spacecraft-level testing, were removed and replaced with panels that had been kept in a nitrogen-purged container. Degradation analysis of the on-board calibrator demonstrated the success of this plan (Chrien et al., 2002). The flight Spectralon panels have degraded on-orbit by no more than a total of 0.5%.

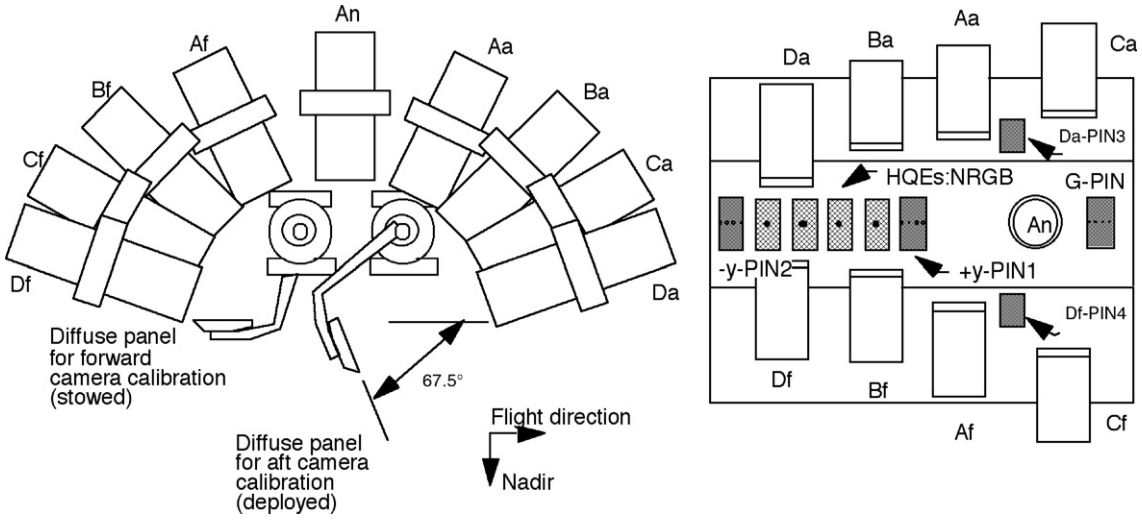

Fig. 1. Schematic of MISR on-board calibrator. Left: Foreward cameras Df–Af and nadir camera, An, view one panel; Aft-cameras Da–Aa and nadir camera, An, view a second panel. Right: Six sets of photodiodes measure panel-reflected sunlight. Each photodiode set has four photodiodes filtered to the MISR passbands.

Not all of the monitoring photodiodes have remained stable on-orbit. The blue-filtered High Quantum Efficient (HQE) device, a light-trapped three detector radiometer, has remained stable to better than 0.5% throughout the mission (Chrien et al., 2002). This diode is therefore used as the primary standard; all other photodiodes are re-calibrated against this standard prior to the bi-monthly data analysis.

3. Level 1B radiometric product

Radiometric data products consist of geo-located radiance images at nadir and off-nadir Earth view angles. These are band-weighted camera-incident radiances, in units of $W\,m^{-2}\,sr^{-1}\,\mu m^{-1}$. Radiances are generated from the instrument output via a linear calibration equation

$$DN - DN_0 = G^* L_0 \quad (1)$$

where

L_0 is the incident spectral radiance, weighted over the total-band response function,

DN is the camera output data number,

DN_0 is the DN offset, unique for each line of data, as determined by an average over the first eight overclock pixel elements, and

G are linear response coefficients which provide the radiometric calibration of a specific pixel.

MISR radiometric coefficients, G, are recomputed following analysis of each bi-monthly OBC experiment. They are then delivered, to the processing center, in a file named the Ancillary Radiometric Product (ARP). Each coefficient set, and thus each ARP file, is valid for the subsequent 2 months, until the next file is delivered. So the ARP is a series of files with a date range of applicability. Level 1B data products contain traceability to the specific ARP file used in its production. This information is found within the metadata field.

MISR Level L1B2 radiances are re-sampled to geolocate and co-register data from the nine cameras and four spectral bands. The final step in converting raw output data into radiances involves an image enhancement algorithm, discussed next.

3.1. Point-spread function

The image of a point object source is always blurred due to diffraction, lens aberrations, and scattering. This output response to a point source is known as the point-spread-function (PSF) for a given optical system. MISR PSF functions have been measured pre-flight, and on-orbit (Bruegge et al., 2004).

For an in-flight determination of the PSF, the derivative of the edge response was taken, using an iceberg edge. The updated response was found to have the same shape, but with a larger halo, as compared to the preflight measurement. That is, the preflight PSFs underestimate the required amount of contrast adjustment. PSF correction, using a simple deconvolution algorithm, is performed on all MISR radiance data products. Following this process, sharp radiance discontinuities can be observed in the presence of contrast edges, as expected.

3.2. Data reprocessing

MISR calibration processes have improved with time. These changes fall into one of two classes: those that update the ARP gain coefficients, and those that modify the L1B processing algorithm. Examples of the first kind are processes that remove radiometric biases. Camera-to-camera adjustments, discussed in a later section, fall into this category. The new calibration process altered the gain coefficients, including those already used to produce radiance data products. For these cases, an updated version of a given ARP is created. During reprocessing, the most recent version of a given ARP, for a given data acquisition period, is used. In this way improvements in the calibration eventually lead to improved radiometric accuracies for the entire MISR archive. The last change to the ARP production software occurred with L1B version 23. Thus, any Level 1B file with that contains the name "F03_0023" has been processed with the latest calibration methodology (where Fxx is a format change to the data product, and _xxx is the version number). This update occurred May 2005, and includes all camera-to-camera bias adjustments.

Changes can also occur in the Level 1B process generator. The decision to implement an image contrast enhancement algorithm (also known as PSF deconvolution) is one example of a L1B process change. This algorithm change was made in 2002. It was the last radiometric calibration algorithm change to the L1B software.

MISR has a reprocessing policy, and all data acquired during the mission have been reprocessed using the final calibration algorithm. Should algorithmic updates be made in the future, information on reprocessing schedules can be found at the NASA/Langley data distribution website, http://eosweb.larc.nasa.gov/PRODOCS/misr/Version/pge1.html. In order to maintain traceability, MISR data users should document the version number of the products they use. This is easily tracked by noting the name of the data product.

4. Preflight testing

For MISR, preflight performance verification and calibration activities were conducted at the camera assembly level. As the camera provides signal detection and analog-to-digital conversion, it is believed that these measurements are representative of performance in the final instrument configuration. (Ambient testing was able to verify performance as an instrument, and on the spacecraft, prior to launch.) The camera-level test plan saved resources, in that testing of the individual cameras could be contained to a small chamber, and testing could be conducted in series as the cameras were assembled. Camera testing did not include processes that govern pixel averaging and square-root encoding, but did provide all needed characterizations.

A pinhole target/collimator assembly was used to determine modulation transfer function (MTF), point-spread function (PSF), camera boresight location, and pixel pointing (distortion) (Hochberg et al., 1996; Korechoff et al., 1996). Radiometric testing utilized a 1.65 m (65″) integrating sphere, calibrated with high quantum efficiency light-trapped photodiodes. Twelve radiometric levels, unique to each spectral band and spanning

the detector dynamic range, were used. A summary of the performance testing results for the MISR cameras is found in Bruegge et al. (1995).

4.1. Spectral calibration

One key pre-flight test was the spectral calibration. Geophysical retrieval algorithms are sensitive to this measurement, and with the MISR design, characterization cannot be repeated on-orbit. Spectral calibration was conducted using a single-pass grating monochromator, xenon arc lamp, and variable width exit slit. Both in-band scans, at 0.5 nm sampling and 2.6 nm resolution, and out-of-band scans, at 19.6 nm resolution and 10 nm sampling, were made for each CCD line array. Testing covered the 400 to 900 nm range, with the response characterization extended from 365 to 1100 nm by use of component-level data. The effective MISR center wavelengths are given in Table 1. This table provides in-band response, as delimited by the 1% response points (Bruegge et al., 2002). A centroid analysis was used in this determination. Also shown are the effective bandwidths, or equivalent square-band response function. These in-band parameters are used to summarize the instrument characteristics, but it must be noted that the Level 1B radiance product includes energy within the total band-pass. Approximately 3% of the camera output comes from signals at wavelengths outside the 1% limits, for a spectrally neutral scene. An adjustment for this out-of-band response is made in the aerosol retrieval algorithm. The final row of the table gives the band-weighted exo-atmospheric solar irradiance. MISR has adopted the solar irradiance model published by the World Radiation Center (Wehrli, 1985, 1986). An EOS agreement selected this model to be used universally by all Terra instruments.

5. On-orbit calibration

5.1. Vicarious calibration

Vicarious calibration (VC) has been used to establish the MISR radiometric scale. VC is the process of measuring ground-reflectance and atmospheric properties over a large, homogeneous test site. The absolute scale is established through an exo-atmospheric solar irradiance database, discussed above. A Terra-common model removes any systematic biases, one instrument to another, which would otherwise be introduced if different models were used. MISR analysis have demonstrated that the Thuillier et al. (1997) and WRC models differ by 2%, −0.3%, 0.2%, and 4.3% respectively, for MISR bands 1–4 (Blue — NIR). This analysis suggests that the uncertainty due to a solar model can lead to measurable instrument biases.

Table 1
MISR in-band spectral parameters

λ_c, nm	$\Delta\lambda$, nm	$E_{0,b}$ [W m^{-2} μm^{-1}]
447	41	1871
558	27	1851
672	20	1525
867	38	969.6

Table 2
VC radiance computation, blue band

Error source	Abs. uncertainty, %
Solar irradiance knowledge	2
Spectralon reflectance knowledge	1.5
Surface reflectance, including errors in geolocation, in-situ sampling, and inhomogeneity	1
Relative surface BRF knowledge	1
Atmosphere characterization	1
Cosine of solar zenith	Negligible
Field instrument SNR	0.1
MISR camera SNR	0.1
Earth–Sun distance	Negligible
Root-sum-squares	3

MISR has made use of several desert playa sites in the southwest US. These data are used to compute top-of-atmosphere (TOA) radiances, within the bandpass of a co-incident on-orbit sensor. A comparison of the VC and sensor radiances provides a calibration, or a validation, of the sensor response. The term vicarious was introduced (Koepke, 1982) to mean "in place of another," or in place of a laboratory calibration. Surface-viewing radiometers characterize an area equal to that of the sensor footprint under test. A homogeneous surface reduces co-registration errors between the effective sensor field-of-view (FOV), and the ground area measured by the field team. It also reduces error due to scene contrast, motion-induced smearing, blurring, and imperfect imaging (point-spread function effects). A second key in-situ dataset is obtained from a tracking sun photometer. These data are used to retrieve aerosol versus wavelength, as well as ozone and column water vapor. These surface and atmosphere data are input to a radiative transfer code, which then computes top-of-atmosphere (TOA) spectral radiances. By modeling the absorption due to ozone and water, a complete TOA spectrum can be computed over the 400–2500 nm wavelength range with fine wavelength sampling. The MISR vicarious calibration approach also makes use of aircraft data. The aircraft counterpart to MISR, AirMISR, is an ER-2 based sensor with 7 m resolution in the nadir at 20 km altitude, and creates images 10 km wide by 9 km long (Diner et al., 1998). Data are used to measure surface homogeneity within the MISR footprint, and to validate camera-to-camera-relative response. Another field instrument unique to the MISR process is the Portable Apparatus for Rapid Acquisition of Bidirectional Observation of the Land and Atmosphere (PARABOLA, Abdou et al., 2000; Bruegge et al., 2000). Data from this instrument measures the playa bidirectional reflectance factor (BRF), and is used within the radiative transfer code.

When a VC experiment is coordinated with the overpass of a satellite, and if there are clear skies and low aerosol conditions, the process yields radiometric accuracies of 3%, as shown for the blue band in Table 2. Errors in the near-infrared band have an additional 1% uncertainty, due to water vapor absorption. The MISR VC process may introduce a small bias in this band, as water vapor was not included in the radiative transfer calculations.

The June 11, 2000 VC provided the first on-orbit absolute calibration of the MISR flight photodiode standards, and in turn that of the instrument. The VC experiment was repeated in

subsequent years, using both nadir and off-nadir viewing angles. A nadir overpass means that the surface target is near the center of the camera's field of view (FOV), whereas an off-nadir overpass places the target closer to the edge of the field (the An camera has a cross-track FOV of ±15°). Results for 5 years of data are shown in Fig. 2. Data for the nadir view, used to calibrate the on-board calibrator, fall within a range of ±3%. Because agreement with MISR has been within the uncertainty of the technique, no updates have been made to the response coefficient of the OBC primary photodiode standard, other than its initial adjustment based upon the 2000 VC experiment.

One interesting finding from the first off-nadir vicarious calibration, June 10, 2002, was a discovery of a 10% bias error in the MISR nadir camera, at the edge of the field. This was traced to a coding error in the Level 1B process generator, and was immediately corrected. Another interesting observation was the effect of out-of-field response on the MISR radiometry. A comparison of MISR data, between uncorrected and PSF-corrected radiances, is 3% for small desert playa, such as Lunar Lake and Ivanpah Playa. This is attributed to the fact that the Nevada desert playas are twice as reflective as the surrounding desert. Thus, PSF correction has proven to be non-negligible even in desert environments.

A summary of the uncertainties for the MISR cameras, are provided in Table 3. At the MISR spatial scales the radiance uncertainties are 4% for the Nevada targets.

This uncertainty is validated with cross-sensor comparisons. Fig. 3 compares the radiances measured by several sensors against the vicarious calibration radiances conducted July 22, 2003. One such comparison is that with AirMISR. This ER2-based instrument is calibrated in the laboratory using a large integrating sphere and a set of high quantum efficiency photodiode standards. AirMISR calibrations performed between October 2002 and May 2004 have a standard deviation of 0.6% or less, depending on spectral band, so the sensor is very stable, and the AirMISR radiometric scale is entirely independent of the MISR scale. Nonetheless, Fig. 3 shows very good agreement

Table 3
MISR absolute calibration uncertainty, VC based approach

Error source	Abs. uncertainty, %	Notes
VC radiance, from Table 2	3	
VC to Blue-HQE transfer	2	
Blue-HQE temporal stability	1	One year time scale, equivalent to VC repeat cycle.
Camera to photodiode view angle BRF ratio	1	
Blue-HQE to operational photodiodes	0.5	Spectral uncertainty of Spectralon on-orbit. Timing errors.
Diffuse panel spatial uniformity	0.5	
Diode SNR	0.1	
Calibration equation functional form	0.1	Negligible in the 0.05–1. Equivalent reflectance range. May be as large as 5% for reflectances <0.02.
Out-of-band response	Negligible	Level 1B1 data products report total-band-weighted incident radiances.
Root-sum-square	4	Radiance error bright land targets

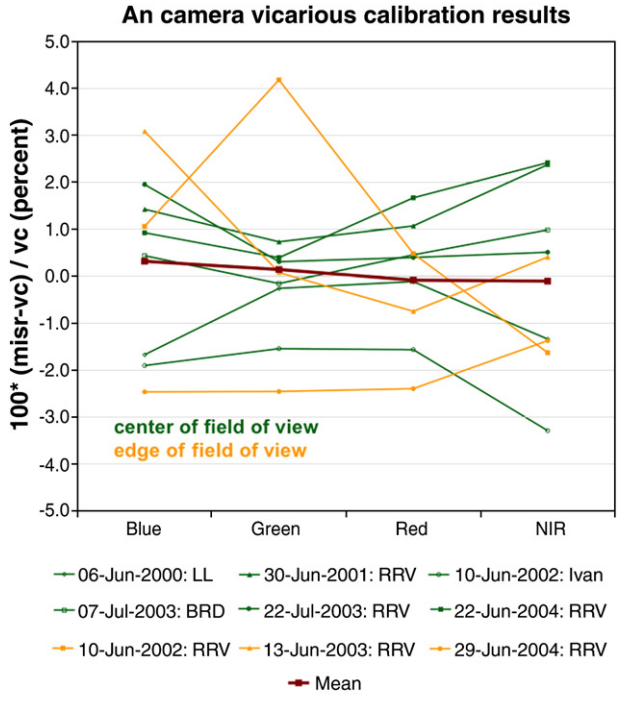

Fig. 2. Average over 5 years' worth of desert playa vicarious calibrations, for the MISR nadir (An) camera. Nadir overpass results are shown as the green lines; off-nadir overpass are shown as the orange lines. For these experiments data were acquired at Lunar Lake (LL), Railroad Valley (RRV), Ivanpah (Ivan), and Black Rock Desert (BRD).

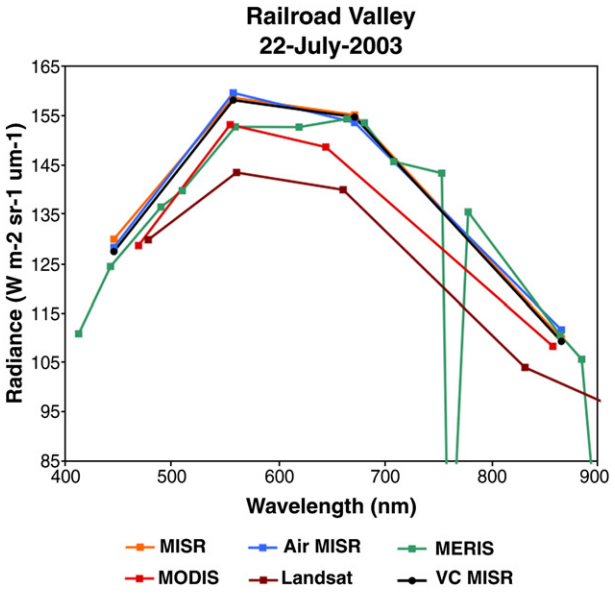

Fig. 3. Measured radiances from Vicarious Calibration data, MISR, MERIS, MODIS, and Landsat. Data were acquired July 22, 2003 at Railroad Valley, Nevada.

between the MISR scale, the VC scale, and AirMISR. MISR is also in good agreement with MERIS in the red and near-infrared, which are the primary bands used in dark-water aerosol retrievals. However, MISR is brighter than MODIS, whose scale is determined from their on-board calibrator, and Landsat-7, whose radiometric scale was set based on preflight data. Independent VC data acquired by the University of Arizona (Thome, 2006) also show a 3% discrepancy with MODIS, similar to our results.

Other investigators have reported the validation of MISR radiometry over very bright targets, such as clouds. Cloud studies have demonstrated that MISR radiance data over very bright targets are consistent with simulations and cross-sensor comparisons (Marchand & Ackerman, 2004).

5.2. Camera-to-camera bias adjustment

As mentioned above, updates to the MISR radiometric calibration process have included an adjustment of the on-board-calibrator, so MISR radiances agree with vicarious calibration experiments. The final process adjustment for MISR was made to correct the camera-to-camera (CTC) response coefficients. Independent data sets were used to validate this process. The first, referred to as the "symmetry" experiment, makes use of those points on the Earth where symmetric camera pairs (e.g., Bf/Ba) view the same location with nearly identical view zenith angles and nearly identical azimuth differences with respect to the Sun. Because most targets should have the same BRF under such conditions, a statistical accumulation of data provides a check on the relative calibration between forward and aft camera pairs. Filters were applied to avoid clouds and ensure scene homogeneity over a 17.6-km area. Averaged results, summarized over a wide range of land scenes observed during different seasons, are shown in the left-hand plot of Fig. 4. The residual asymmetry may arise from uncorrected differences in the BRFs of the Spectralon panels. A set of channel-by-channel correction factors was derived, and their application leads to the plot on the right-hand side of Fig. 4.

The symmetry technique cannot tell whether a fore-aft asymmetry is due to the radiance in one camera being too bright, the other being too dark, or something in between. Consequently, lunar observations were used to distribute the bias adjustments. The lunar-view experiment occurred on April 2003 during the "reverse somersault" which the Terra spacecraft performed during this maneuver. Here all nine cameras swept past the lunar disk at the same face-on observation angle. CTC residuals relative to the mean value in each spectral band are shown in the left-hand plot of Fig. 5. Application of the gain correction factors derived to make the adjustments shown in Fig. 4 results in the right-hand plot of Fig. 5. Overall, a slight improvement in the channel-by-channel residuals is observed. We also found that the same adjustment factors reduced the off-nadir band-to-band (BTB) differences in MISR/AirMISR radiance ratios. The CTC correction factors were typically small, usually 1% or less. The largest adjustment was applied to the Bf camera, particularly in the near-infrared band, where a 2.5% reduction in radiance was applied.

The net effect of CTC corrections on aerosol optical depth was estimated by randomly selecting a few orbits containing

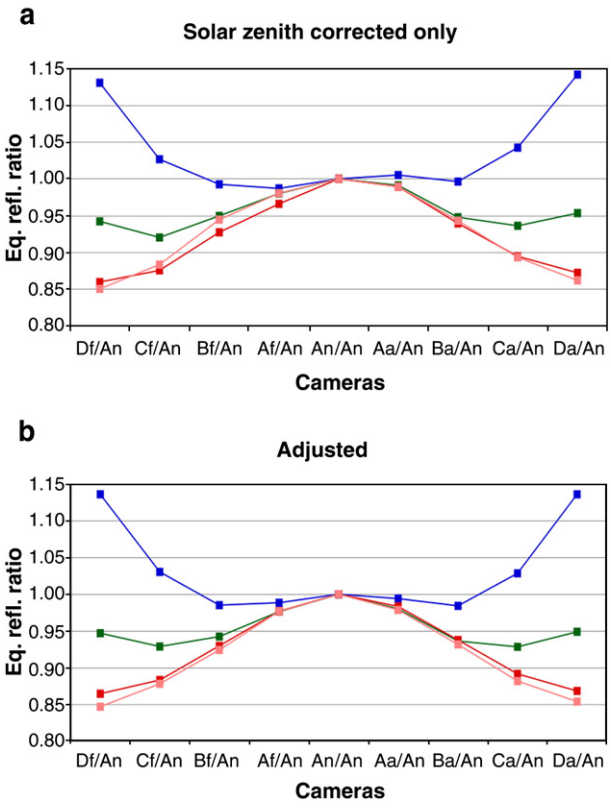

Fig. 4. Left: Plot of "symmetry" data acquired over land. The curves are expected to be symmetric fore-aft. Due to the 7-minute time interval between the Df and Da views of a particular scene, a correction for solar zenith angle was applied. Right: Effect of including CTC correction factors. Data for each of the MISR wavelengths are color-coded as blue, green, red, and peach.

dark-water retrievals and regressing the results obtained with and without the corrections. The results show an overall reduction averaging of 0.02 in aerosol optical depth. (Diner et al., 2004). This is about one-third of the difference between MISR and AERosol RObotic NETwork (AERONET) results for dark-water, low aerosol optical thickness scenes, showing that there is sensitivity to these refinements.

6. Validation studies

6.1. Calibration over dark-water

Validation of MISR radiometry over dark ocean sites has added importance in that instrument artifacts, such as additive stray-light or electronic biases, if present, would lead to large radiometric errors in the measure of incident radiance. These could be as large or larger than the actual radiance to be measured. MISR has 14-bit quantization, and therefore has roughly 16,384 gray levels. (The finite video offset and square-root encoding reduces this by about 300 counts.) A signal of 0.02 in equivalent reflectance results in an output DN of from 300 to 800 DN, depending on the detector. For dark targets, errors of 30 DN may begin to affect radiometric accuracy significantly. Therefore, validation of MISR radiometry over dark ocean sites is more challenging than over bright land targets. Although dark-water vicarious calibrations can be conducted, they are not routine. For

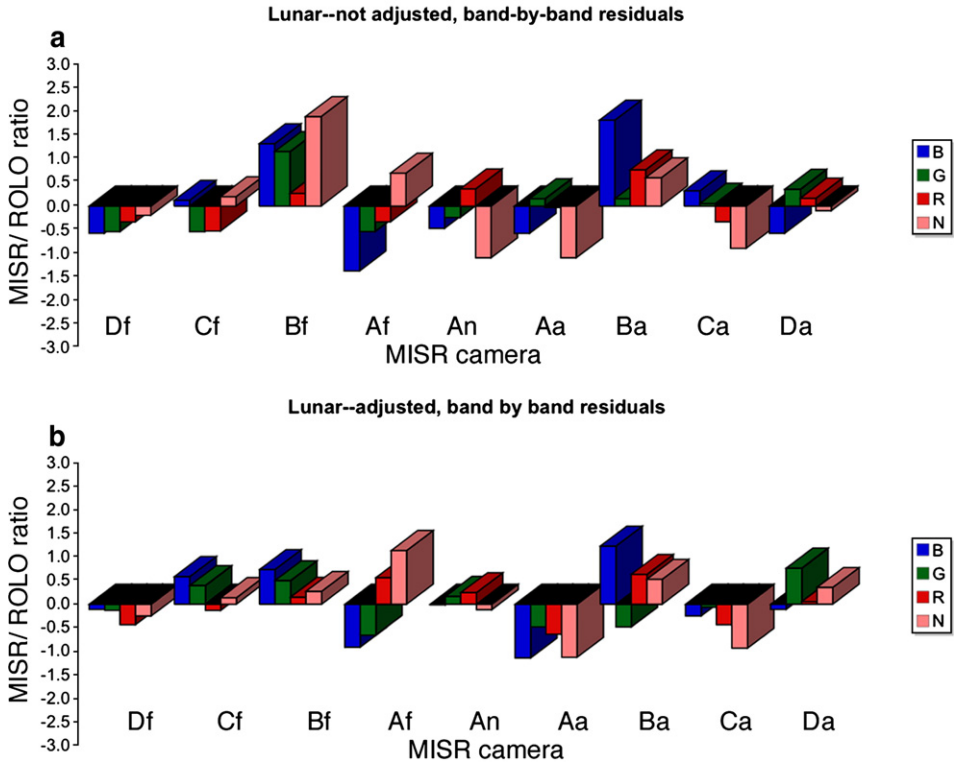

Fig. 5. Left: Band-by-band residuals between MISR radiances and values obtained from the RObotic Lunar Observatory (ROLO) model (Kieffer et al., 2002). The absolute offset between the MISR radiometric scale and the ROLO model of about 5% has been subtracted out, so that this plot shows the camera-by-camera residuals about this offset for each spectral band. Right: Residuals obtained after application of the CTC correction factors. Data for each of the MISR wavelengths are color-coded as blue, green, red, and peach.

these cases the atmospheric contribution to top-of-atmosphere radiance dominates the surface term, and the process of computing top-of-atmosphere radiances from in-situ measurements is less certain. Further, when comparisons are made with nadir-only viewing sensors, the data are frequently contaminated with glint. These cases must be eliminated in the analysis as the large radiance gradient of these scenes makes data comparisons less reliable. Following this screening, patterns repeated over many well-constrained cases lend confidence to the results, at a few percent accuracy.

A dark-target calibration of MISR has been reported by Kahn et al. (2005). Here data from the AERONET, in conjunction with an ocean reflectance model and radiative transfer model are used to predict top-of-atmosphere radiances, and compared to MISR and other sensors. The Terra/Moderate-Resolution Imaging Spectro-radiometer (MODIS) instrument is one possible cross-comparison source. Co-located on the same platform, MODIS and MISR view a scene simultaneous in time and with similar bandpasses. The results of one such study is given in Fig. 6. These data were acquired at different locations near Lanai and Midway islands. Cases 1 water sites were selected, isolated from continental runoff. Using the measurements from Morel and Maritorena (2001), the surface reflectance was modeled as 0.03, 0.007, 0.002, and 0.0007 in the MISR blue, green, red, and near-infrared bands. AERONET data was used to retrieve aerosol spectral optical thickness, size distribution, and single-scattering albedo, along with in situ wind measurements. Conclusions are strongest in the red and green bands, but have a greater uncertainty in the near-infrared. MISR nadir-view and MODIS low-light-level absolute reflectance differ by about 4% in the blue and green bands, with MISR having the higher values. In the red, MISR agrees with MODIS Band 14 to better than 2%, whereas MODIS Band 1 is significantly lower and appears as an outlier. This is significant because Band 1 is among those used for MODIS aerosol retrievals, even over ocean. Compared to the AERONET-constrained model, the MISR aft-viewing cameras report reflectances too high by several percent in the blue, green, and possibly the red. These results are consistent with the finding reported elsewhere in this publication, and demonstrate that ocean-reported radiances are valid and accurate to within 4% for these nadir observations.

6.2. Operational processes in the extended mission era

During the first four MISR post-launch years, many focused studies were conducted, as reported above. These included lunar-views, dark-water studies, and multi-sensor cross-comparisons over Nevada desert targets. With these the quality of the MISR instrument calibration has been verified, along with the calibration procedures. These observations have led us to conclude that the MISR on-board calibrator is stable, and that MISR response degradation has been properly corrected using the on-board calibrator.

Fig. 7 shows the results of 6 years of MISR response, as determined from the OBC. These data show a steady decline in response, of approximately 2% per year, for the nadir camera.

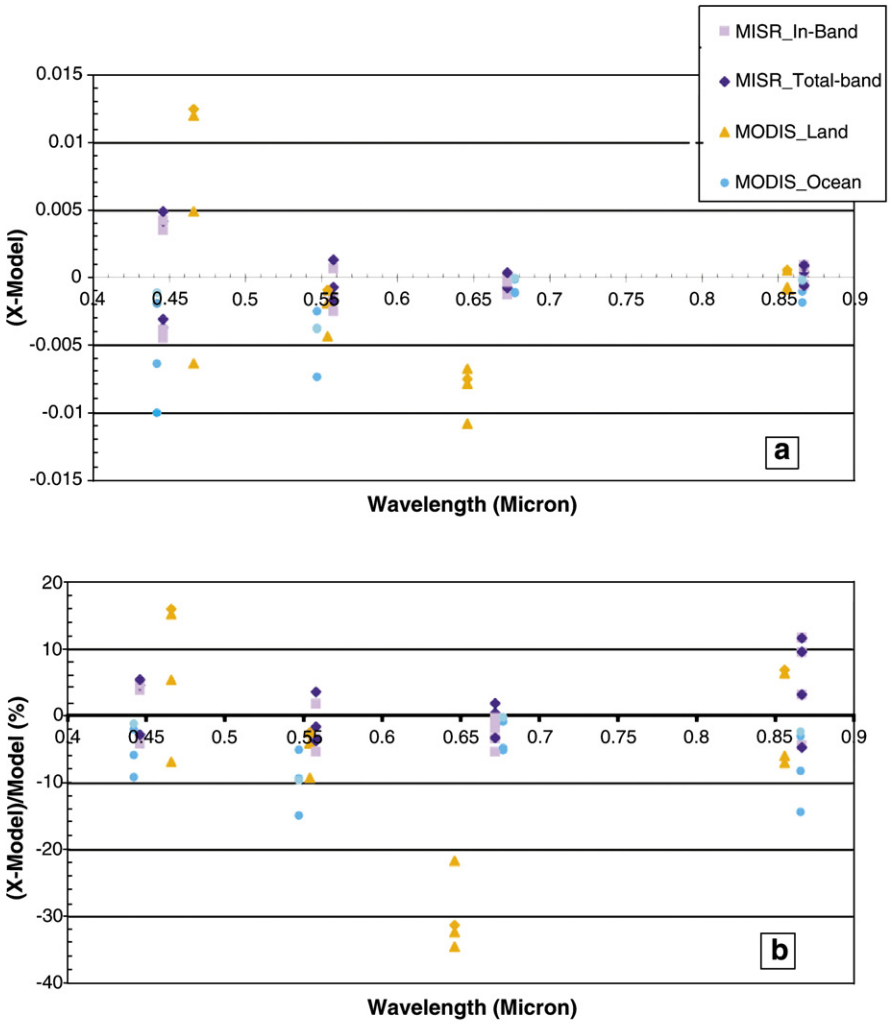

Fig. 6. Comparison of MISR and MODIS radiances over dark-water sites with VC results calculated using surface reflectance and AERONET data, as a function of wavelength. Good agreement is observed between the MISR and MODIS ocean measurements and the model.

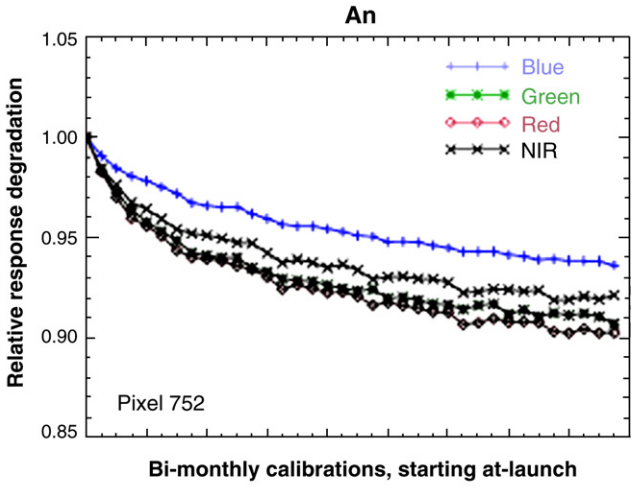

Fig. 7. January 2006 summary of MISR trend history. Data points represent response degradation at bi-monthly intervals, as normalized to the first determination.

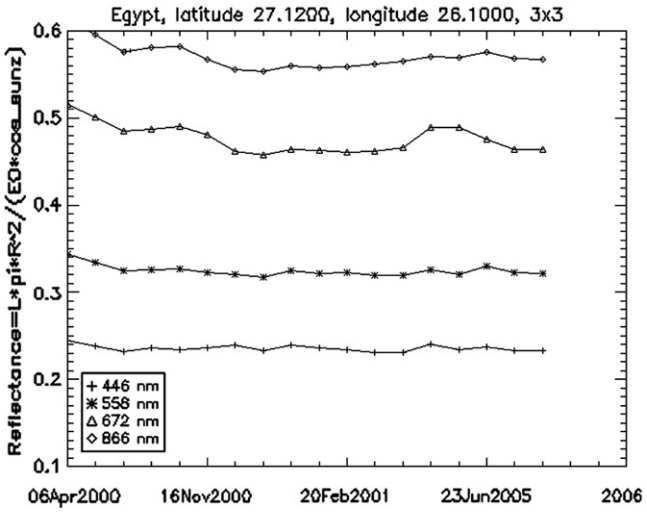

Fig. 8. MISR radiance observations over the Egypt-1 desert site and normalized for sun-zenith illumination.

Results for the other cameras are similar in appearance (see http://www-misr.jpl.nasa.gov/mission/valwork/cal_reports/arp.html#trend). Application of the OBC-derived calibration coefficients compensate for these changes.

To confirm OBC stability, MISR also routinely monitors radiance over Sahara desert sites. The Egypt-1 site, as selected by Cosnefroy et al. (1996), is known to be lacking in vegetation, and has low aerosol amounts for much of the year. MISR observations of this site are shown in Fig. 8. These data are normalized by earth–sun distance, and the cosine of the solar zenith illumination angle. For each of these sites, the standard deviation of radiances, within a 3×3 footprint 1.1 km in size is less than 1%. Although there is some reflectance variability from one observation to the next, on the order of 0.02, the long-term trend appears stable. This analysis demonstrates the effectiveness of the bi-monthly OBC calibration approach, and checks for degradation of the OBC itself. Using these two techniques, MISR's radiometric calibration will be maintained into the future.

7. Conclusions

The MISR radiometric scale has been set using a vicarious calibration experiment, and is maintained by use of an on-board calibrator. The Spectralon panels and HQE-blue photodiode have remained stable to within 0.5%. The radiometric stability of the MISR Spectralon panels is attributed to the vacuum-baking process, and to the change out of the panels, following testing, for environmentally protected panels. Lessons from 4 years of active validation of the radiometric scale have taught us that these studies must span the range of conditions used by the data users. For MISR, validations have included cross-sensor comparisons, lunar-views, a dark-water case study, and a statistical analysis of Earth data. Studies were conducted over a range of illumination levels, cross-track view angles, and scene contrasts.

MISR and MODIS radiance data agree to within a 4% uncertainty, providing that the MODIS "land" channels are used over land and the MODIS "ocean" channels are used over ocean. The agreement of the ocean values, using the MODIS ocean channels, provides a validation of MISR radiometry at these low-light levels. The studies discussed here confirm MISR absolute accuracy of 4% for bright scenes, 10% for dark ocean cases, and a 1% camera- and band-relative uncertainties.

MISR is currently in its extended mission phase, having acquired science data for 6 years. As both the instrument and on-board calibrator have remained stable on-orbit, the mission is continuing with a simplified calibration plan. It now consists of bi-monthly deployments of the on-board calibrator and analysis of radiances reported over stable desert sites. With these processes, MISR calibration will be maintained through the duration of the mission.

Acknowledgments

The work described in this paper is being carried out at the Jet Propulsion Laboratory, California Institute of Technology, under contract with the National Aeronautics and Space Administration. MISR data products are processed and made available by the Atmospheric Sciences Data Center, Langley Research Center.

References

Abdou, W., Bruegge, C., Helmlinger, M., Conel, J., Pilorz, S., & Gaitley, B. (2002). Vicarious calibration experiment in support of the Multi-angle Imaging SpectroRadiometer (MISR). *IEEE Transactions on Geoscience and Remote Sensing*, *40*(7), 1500−1511.

Abdou, W. A., Helmlinger, M. C., Conel, J. E., Pilorz, S., Bruegge, C. J., Gaitley, B. J., et al. (2000). Ground measurements of surface bidirectional reflectance factor (BRF) and hemispherical directional reflectance factor (HDRF) using the portable Apparatus for Rapid Acquisition of Bidirectional observation of the land and atmosphere (PARABOLA III). *Journal of Geophysical Research*, *106*, 11967−11976.

Bruegge, C. J., Abdou, W. A., Diner, D. J., Gaitley, B. J., Helmlinger, M. C., Kahn, R. A., et al. (2004). Validating the MISR radiometric scale for the ocean aerosol science communities. In S. A. Morain & A. M. Budge (Eds.), *Post-launch calibration of satellite sensors (103–115),* Leiden, Netherlands: A.A. Balkema Publishers.

Bruegge, C. J., Chrien, N. L., Ando, R. R., Diner, D. J., Abdou, W. A., Helmlinger, M. C., et al. (2002). Early validation of the Multi-angle Imaging SpectroRadiometer (MISR) Radiometric Scale. *IEEE Transactions on Geoscience and Remote Sensing*, *40*(7), 1477−1492.

Bruegge, C., Chrien, N., & Haner, D. (2001). A Spectralon BRF data base for MISR calibration applications. *Remote Sensing of Environment*, *76*, 354−366.

Bruegge, C. J., Duval, V. G., Chrien, N. L., & Korechoff, R. P. (1995). MISR instrument development and test status. *Advanced and next-generation satellites. Proc. EUROPTO/ SPIE 2538, 92–103, Paris, France, 25–28 September.*

Bruegge, C. J., Helmlinger, M. C., Conel, J. E., Gaitley, B. J., & Abdou, W. A (2000). PARABOLA III: A sphere-scanning radiometer for field determination of surface anisotropic reflectance functions. *Remote Sensing Reviews*, *19*, 75−94.

Bruegge, C., Stiegman, A., Rainen, R., & Springsteen, A. (1993). Use of Spectralon as a diffuse reflectance standard for in-flight calibration of earth-orbiting sensors. *Optical Engineering*, *32*(4), 805−814.

Chrien, N., Bruegge, C., & Ando, R. (2002). Multi-angle Imaging Spectro-Radiometer (MISR) on-board calibrator (OBC) in-flight performance studies. *IEEE Transactions on Geoscience and Remote Sensing*, *40*(7), 1493−1499.

Cosnefroy, H., Briottet, X., & Leroy, M. (1996). Selection and characterization of Sahara and Arabian desert sites for the calibration of optical satellite sensors. *Remote Sensing of Environment*, *58*(1), 101−114.

Diner, D. J., Abdou, W. A., Bruegge, C. J., Conel, J. E., Crean, K. A., Gaitley, B. J., et al. (2001). MISR aerosol optical depth retrievals over southern Africa during the SAFARI-2000 dry season campaign. *Geophysical Research Letters*, *28*, 3127−3130.

Diner, D. J., Barge, L. M., Bruegge, C. J., Chrien, T. G., Conel, J. E., Eastwood, M. L., et al. (1998). The Airborne Multi-angle SpectroRadiometer (AirMISR): Instrument description and first results. *IEEE Transactions on Geoscience and Remote Sensing*, *36*, 1339−1349.

Diner, D. J., Kahn, R. A., Bruegge, C. J., Martonchik, J. V., Abdou, W. A., Gaitley, B. J., et al. (2004). Refinements to MISR's radiometric calibration and implications for establishing a climate-quality aerosol observing system. *SPIE Proceedings Series*, *5652*, 57−65.

Diner, D. J., Martonchik, J. V., Kahn, R. A., Pinty, B., Gobron, N., Nelson, D. L., et al. (2005). Using angular and spectral shape similarity constraints to improve MISR aerosol and surface retrievals over land. *Remote Sensing of Environment*, *94*, 155−171.

Hochberg, E. B., White, M. L., Korechoff, R. P., & Sepulveda, C. A. (1996). Optical testing of MISR lenses and cameras. *Optical Spectroscopic Techniques and Instrumentation for Atmospheric Space ResearchProc. SPIE, Denver, Colorado, 5–9 August*, *vol. 2830*. (pp.).

Kahn, R., Banerjee, P., & McDonald, D. (2001). The sensitivity of multi-angle imaging to natural mixtures of aerosols over ocean. *Journal of Geophysical Research*, *103*(D24), 32195−32213.

Kahn, R., Banerjee, P., McDonald, D., & Diner, D. J. (1998). Sensitivity of multiangle imaging to aerosol optical depth and to pure-particle size distribution and composition over ocean. *Journal of Geophysical Research*, *103*(D24), 32195−32213.

Kahn, R., Li, W. -H., Bruegge, C., Martonchik, J., Diner, D., Gaitley, B., et al. (2005). MISR low-light-level calibration, and implications for aerosol retrieval over dark water. *Journal of the Atmospheric Sciences*, *62*(4), 1032−1062.

Kalashnikova, O.V. & Kahn, R.A. (in press). The ability of multi-angle remote sensing observations to identify and distinguish mineral dust types: Part 2. Sensitivity over dark water. *Journal of Geophysical Research*.

Kieffer, H. H., Jarecke, P., & Pearlman, J. (2002). Initial Lunar Calibration Observations by the EO-1 Hyperion Imaging Spectrometer. *Proceedings of SPIE*, *4480*, 247−258.

Koepke, P. (1982). Vicarious satellite calibration in the solar spectral range by means of calculated radiances and its application to Meteosat. *Applied Optics*, *21*(15), 2845−2854.

Korechoff, R., Kirby, D., Hochberg, E., Sepulveda, C., & Jovanovic, V. (1996). Distortion calibration of the MISR linear detectors. *Earth observing system., proc. SPIE 2820, Denver, Colorado, 5–9 August*.

Marchand, R., & Ackerman, T. (2004). Evaluation of radiometric measurements from the NASA Multiangle Imaging Spectroradiometer (MISR): Two- and three-dimensional radiative transfer modeling of an inhomogeneous stratocumulus cloud deck. *Journal of Geophysical Research*, *109*(D18), D18208.

Martonchik, J., Diner, D. J., Crean, K. A., & Bull, M. A. (2002). Regional aerosol retrieval results from MISR. *IEEE Transactions on Geoscience and Remote Sensing*, *40*, 1520−1531.

Morel, A., & Maritorena, S. (2001). Bio-optical properties of oceanic waters: A reappraisal. *Journal of Geophysical Research*, *106*, 7163−7180.

Stiegman, A. E., Bruegge, C. J., & Springsteen, A. W. (1993). Ultraviolet stability and contamination analysis of Spectralon diffuse reflectance material. *Optical Engineering*, *32*(4), 799−804.

Thome, K. (2006). Private communication.

Thuillier, G., Herse, M., Simon, P. C., Labs, D., Mandel, H., & Gillotay, D. (1997). Observation of the UV solar spectral irradiance between 200 and 350 nm during the ATLAS 1 mission by the SOLSPEC spectrometer. *Solar Physics*, *171*, 283−302.

Wehrli, C. (1985, July). *Extraterrestrial solar spectrum.* Davos-Dorf, Switzerland: WRC Publication 615.

Wehrli, C. (1986, October). Revised instruction manual on radiation instruments and measurements. In C. Froehlich, & J. London (Eds.), *WCRP Publications Series*, *vol. 7*. (pp. 119−126)Davos, Switzerland: WCRP WMO ITD No. 149.